Polarization gradient: exploring an original route for optical trapping and manipulation

Gabriella Cipparrone,[1,*] Ibis Ricardez-Vargas,[2] Pasquale Pagliusi,[1] and Clementina Provenzano[1]

[1] *LiCryL Laboratory CNR-INFM, Excellence Centre CEMIF.CAL and Physics Department, University of Calabria, Ponte P. Bucci, Cubo 33B, 87036 Rende (CS), Italy*

[2] *Departamento de Física Teórica, Instituto de Física, Universidad Nacional Autónoma de México, A. P. 20-364, México D.F. 01000, México.*

**cipparrone@fis.unical.it*

Abstract: We report a study of the capabilities of an optical tweezer based on polarization gradient. We use a light polarization pattern that is able to simultaneously exert forces and torques in opposite directions depending on the particle's position. It allows to perform oscillatory displacements and control the sense of rotation of several particles inside a uniformly illuminated region. Unconventional trapping of spinning particles in circularly polarized fringes has been observed, which suggests the involvement of hydrodynamic forces.

OCIS codes: (090.2880) Holography; (350.4855) Optical tweezers or optical manipulation; (160.3710) Liquid crystals.

References and links

1. A. Ashkin, "Acceleration and trapping of particles by radiation pressure," Phys. Rev. Lett. **24**(4), 156–159 (1970).
2. D. G. Grier, "A revolution in optical manipulation," Nature **424**(6950), 810–816 (2003).
3. J. R. Moffitt, Y. R. Chemla, S. B. Smith, and C. Bustamante, "Recent advances in optical tweezers," Annu. Rev. Biochem. **77**(1), 205–228 (2008).
4. M. E. J. Friese, T. A. Nieminen, N. R. Heckenberg, and H. Rubinsztein-Dunlop, "Optical alignment and spinning of laser-trapped microscopic particles," Nature **394**(6691), 348–350 (1998).
5. A. T. O'Neil, I. MacVicar, L. Allen, and M. J. Padgett, "Intrinsic and extrinsic nature of the orbital angular momentum of a light beam," Phys. Rev. Lett. **88**(5), 053601 (2002).
6. V. Garcés-Chávez, D. McGloin, H. Melville, W. Sibbett, and K. Dholakia, "Simultaneous micromanipulation in multiple planes using a self-reconstructing light beam," Nature **419**(6903), 145–147 (2002).
7. R. L. Eriksen, P. J. Rodrigo, V. R. Daria, and J. Glückstad, "Spatial light modulator-controlled alignment and spinning of birefringent particles optically trapped in an array," Appl. Opt. **42**(25), 5107–5111 (2003).
8. S. K. Mohanty, K. D. Rao, and P. K. Gupta, "Optical trap with spatially varying polarization: application in controlled orientation of birefringent microscopic particle(s)," Appl. Phys. B **80**(6), 631–634 (2005).
9. D. Preece, S. Keen, E. Botvinick, R. Bowman, M. Padgett, and J. Leach, "Independent polarisation control of multiple optical traps," Opt. Express **16**(20), 15897–15902 (2008), http://www.opticsinfobase.org/oe/abstract.cfm?URI=oe-16-20-15897.
10. L. Allen, S. M. Barnett, and M. J. Padgett, Optical Angular Momentum (Institute of Physics Publishing, Bristol, 2003).
11. Y. Roichman, B. Sun, Y. Roichman, J. Amato-Grill, and D. G. Grier, "Optical forces arising from phase gradients," Phys. Rev. Lett. **100**(1), 013602 (2008).
12. L. Nikolova, and T. Todorov, "Diffraction efficiency and selectivity of polarization holographic recording," Opt. Acta (Lond.) **31**, 579–588 (1984).
13. S. G. Cloutier, "Polarization holography: orthogonal plane-polarized beam configuration with circular vectorial photoinduced anisotropy," J. Phys. D Appl. Phys. **38**(18), 3371–3375 (2005).
14. S. M. Barnett, "Optical angular momentum flux," J. Opt. B Quantum Semiclassical Opt. **4**(2), 361 (2002).
15. R. Zambrini, and S. M. Barnett, "Angular momentum of multimode and polarization patterns," Opt. Express **15**(23), 15214–15227 (2007), http://www.opticsinfobase.org/oe/abstract.cfm?URI=oe-15-23-15214.
16. S. Juodkazis, S. Matsuo, N. Murazawa, I. Hasegawa, and H. Misawa, "High–efficiency optical transfer of torque to a nematic liquid crystal droplet," Appl. Phys. Lett. **82**(26), 4657–4659 (2003).
17. N. Murazawa, S. Juodkazis, and H. Misawa, "Characterization of bipolar and radial nematic liquid crystal droplets using laser-tweezers," J. Phys. D Appl. Phys. **38**(16), 2923–2927 (2005).
18. C. Manzo, D. Paparo, L. Marrucci, and I. Jánossy, "Light-induced rotation of dye-doped liquid crystal droplets," Phys. Rev. E Stat. Nonlin. Soft Matter Phys. **73**(5), 051707 (2006).

#119442 - $15.00 USD Received 2 Nov 2009; revised 10 Dec 2009; accepted 7 Feb 2010; published 11 Mar 2010

19. S. I. Rubinow, and J. B. Keller, "The transverse force on a spinning sphere moving in a viscous fluid," J. Fluid Mech. **11**(03), 447–459 (1961).
20. G. K. Batchelor, An Introduction to Fluid Mechanics (Cambridge University Press, Cambridge, 1967)

1. Introduction

Since its inception [1] the field of optical tweezers has grown tremendously. New techniques that use forces and torques exerted by carefully sculpted light beams improved the level of access and control needed to look at new opportunities of fundamental and applied research in several branches of science [2,3].

Recent studies in the fields of optical manipulation have led to alternative methodologies [2,3] aimed to overcome the limitations in resolution and accuracy, and to manipulate more complex systems. Very suggestive techniques based on properly shaped wavefronts have been investigated to optimize the light's ability to exert forces and torques by means of the transfer of both linear and angular momentum [2–6]. Although very sophisticated methods to develop multiple and multifunctional optical traps have been proposed [7–9], which are able to control the rotation and orientation of birefringent particles exploiting the polarization of the light, the intensity gradient is at the basis of their conventional trapping operation principle and none of them make evidence of optical force gradients based on the vectorial nature of the light. Even in the case of the experiment exploiting pure polarization patterns [8], no prediction or observations of new trapping and manipulation capabilities coming from polarization gradients are reported. Only recently, the studies of the helical modes [5,6,10] suggested that a phase gradient can be also used for optical manipulation [11].

Here we demonstrate how a polarization gradient, created via vectorial holography [12], offers new capabilities for optical trapping and manipulation. We propose an experiment, which enables to verify the presence of optical forces related to the polarization gradient and hydrodynamic forces on rotating particles originating from this optical force field.

2. Vectorial holography

Polarization (or vectorial) holography relies on the interference of asymmetrically polarized beams [12]. Among several configurations, here we consider the interference of two beams with orthogonal linear polarizations, *s* and *p* respectively, and equal intensity, at a small angle θ, see Fig. 1(a).

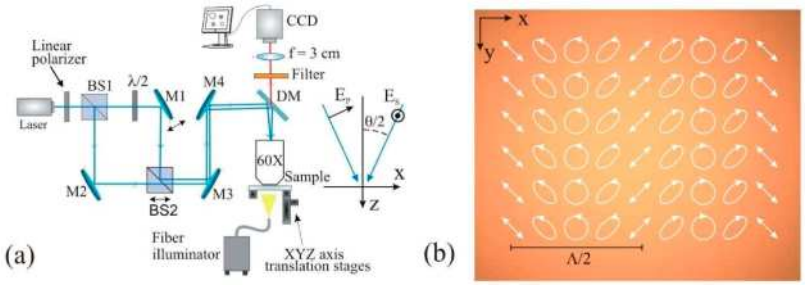

Fig. 1. Experimental set up and geometry. (a) A *s*-polarized Argon ion laser beam at λ=488nm, is sent into a Mach Zehnder interferometer. The half-wave plate (λ/2) in one of the two arms converts into *p* the polarization of the beam propagating in it. The two s- and p- polarized beams are directed towards the 60x microscope objective by a dichroic mirror (DM), and interfere on the sample. The spatial periodicity of the resulting polarization pattern can be tuned by shifting the beamsplitter BS2. The piezoelectric mirror mount M1, driven by an arbitrary function generator, enables the movement of the polarization pattern along the x-axis. The sample position is adjusted via a xyz-translation stage. A computer controlled CCD camera and a fiber illuminator have been used to image the sample. (b) The polarization pattern generated in the sample plane (xy-plane) by the interference of the *s*- and *p*-polarized beams, propagating in xz-plane at angle θ/2 with respect to the z-axis.

The resulting optical electric field and intensity profile in a homogenous and isotropic medium are [12,13]:

#119442 - $15.00 USD Received 2 Nov 2009; revised 10 Dec 2009; accepted 7 Feb 2010; published 11 Mar 2010

$$\vec{E} = \vec{E}_p + \vec{E}_s = E_o\left(\cos\frac{\theta}{2}\exp(-i\delta)\hat{x} + \exp(i\delta)\hat{y} - \sin\frac{\theta}{2}\exp(-i\delta)\hat{z}\right)\exp(-i\beta) \quad (1)$$

$$I = \left(\vec{E}_p + \vec{E}_s\right)\cdot\left(\vec{E}_p + \vec{E}_s\right)^* = E_0^2\left(\cos^2\theta + 1 + \sin^2\theta\right) = 2E_0^2 \quad (2)$$

where $\beta = \frac{2\pi n}{\lambda}\cos\frac{\theta}{2}z$, $\delta = \frac{2\pi n}{\lambda}\sin\frac{\theta}{2}x = \frac{\pi}{\Lambda}x$ and $\Lambda = \frac{\lambda}{2n\sin\theta/2}$, with n refractive index, is the spatial periodicity of the pattern. In such a case, no intensity modulation occurs in the interference region. The purely vectorial polarization pattern consists of an elliptical polarization state of constant inclination ($\pm 45°$), whose ellipticity is continuously modulated, from −1 to 1, versus the x-coordinate, see Fig. 1(b).

To evaluate the mechanical properties of such a light field, the linear and angular momentum densities are calculated. The linear momentum density carried by the light in the interference region can be evaluated by:

$$\vec{g} = \frac{1}{c^2}\mathrm{Re}\left\{\vec{E}^* \times \vec{H}\right\} = \frac{1}{c^2}\sqrt{\frac{\varepsilon}{\mu}}E_0^2\left(\hat{y}\sin\theta\cos\frac{2\pi x}{\Lambda} + \hat{z}2\cos\frac{\theta}{2}\right) \quad (3)$$

where the magnetic field in the interference region is calculated from the Eq. (1):

$$\vec{H} = \vec{H}_p + \vec{H}_s = \frac{i}{\omega\mu}\left(\nabla\times\vec{E}_p + \nabla\times\vec{E}_s\right) = \\ = \sqrt{\frac{\varepsilon}{\mu}}E_o\left(-\cos\frac{\theta}{2}\exp(i\delta)\hat{x} + \exp(-i\delta)\hat{y} - \sin\frac{\theta}{2}\exp(i\delta)\hat{z}\right)\exp(-i\beta). \quad (4)$$

Beside the usual longitudinal z-component, a transverse y-component occurs for $\vec{g}$, which is spatially modulated versus the x-coordinate along with the polarization pattern (see Fig. 2(a)), and is responsible for the transverse force field along $\hat{y}$ (see Fig. 2(b)).

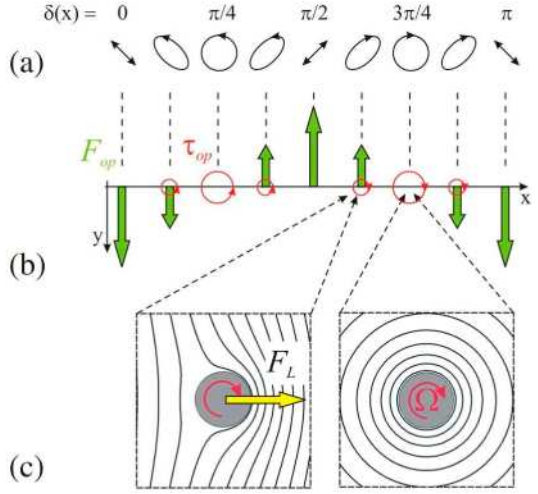

Fig. 2. (a) Scheme of the polarization pattern versus the half phase difference δ(x). (b) The optical torque τ_{op} (in red) and the y-component of the optical force F_{op} (in green) felt by a spherical particle with diameter lower than Λ/2. (c) Symmetric streamlines occur around the particle, rotating with angular velocity Ω, when it is centred on the circularly polarized fringe. Asymmetric streamlines occur when the particle is centred on an elliptically polarized fringe, due to its linear velocity along the y-axis, and the lift force F_L arises along the x-axis, working as a restoring force for the rotating particle toward the regions with circular polarization.

The angular momentum density follows from the linear momentum density $\vec{g}$ as [14,15]:

$$\vec{j} = \vec{r}\times\vec{g} \quad (5)$$

#119442 - $15.00 USD Received 2 Nov 2009; revised 10 Dec 2009; accepted 7 Feb 2010; published 11 Mar 2010

whose z component is:

$$j_z = \frac{1}{c^2}\sqrt{\frac{\varepsilon}{\mu}}E^2(\sin\theta)\,x\cos\frac{2\pi x}{\Lambda} \tag{6}$$

The total angular momentum J_z, obtained by the integration of j_z over the interference region, exhibits two contributions: an orbital component associated with the spatial distribution of the wave and a spin component associated with the ellipticity of the light.

When a particle is located in the optical field (1) and electromagnetically coupled with it (i.e., through absorption, birefringence, shape), transfer of linear and angular momentum from light to matter may occurs depending on the particle position, shape and dimension. Therefore an optical force

$$\vec{F}_{op} = Q\frac{2A}{c}[\hat{y}\sin\theta\iint\cos\frac{2\pi x}{\Lambda}dxdy + \hat{z}2\cos\frac{\theta}{2}\iint dxdy] \tag{7}$$

and torque

$$\vec{\tau}_{op} = Q'\frac{2A}{c}\hat{z}\sin\theta\iint x\cos\frac{2\pi x}{\Lambda}dxdy \tag{8}$$

arise on the particle after integration of $\vec{g}$ and $\vec{j}$ over the particle area in the xy-plane, where Q and Q' are the parameters accounting for the linear and angular momentum transferred to the particle and A is the intensity of the light, see Fig. 2(b).

3. Experiment and results

This scenario has been experimentally explored using an emulsion of a nematic liquid crystal (LC) in distilled water, a system already adopted for optical manipulation experiments [16–18]. Spherical droplets of LC with diameter ranging from 1 to 20μm can be obtained, which are transparent in the whole visible range. A relevant aspect of this system is that droplets with radial and bipolar nematic configuration can be found in the same emulsion [16]. The sole optical linear momentum can be transferred to radial droplets, which are optically isotropic with an average refractive index higher than that of water. On the other hand, both linear and angular momentum can be transferred to bipolar droplets, which are optically anisotropic [16,17]. These features enable to test different dynamical behaviours, maintaining almost constant the experimental conditions and the materials parameters, i.e. the average refractive index of the droplets.

Two Argon laser beams at λ=488nm, with orthogonal *s* and *p* linear polarizations, are directed towards a 60x microscope objective and interfere on the sample (Fig. 1(a)). The beams entering the objective and the illuminated area of the sample are about 2mm and 40μm in diameter, respectively. The intensity in the interference region is virtually uniform (~100mW/cm^2) and the spatial periodicity of the polarization pattern Λ ~10μm (Fig. 1(b)). A piezoelectric actuated mirror mount allows to move the mirror M1 of the Mach-Zehnder interferometer to shift the polarization fringes.

Particles with a diameter d≤Λ/2, i.e. in the range 1-5μm, experience a modulated y-component of the optical force $F_{op,y}$ with a calculated amplitude ~1pN, according to Eq. (7).

Let us consider a transparent isotropic particle, i.e. a radial droplet, at rest in a circular polarization fringe. No transfer of angular momentum occurs ($\vec{\tau}_{op} = \vec{0}$) implying null angular velocity $\vec{\Omega}$. The translation of the polarization pattern induces a displacement of the particle along $\pm\hat{y}$, due to the birth of the $F_{op,y}$. In Fig. 3, the dynamics of a radial LC droplet with d=2μm is reported. Starting from a position $x_0 = \pm m\Lambda/4$, with m odd, corresponding to a circular polarization fringe (i.e., $F_{op,y}(x_0) = 0$), when the fringes are moved along $\pm\hat{x}$ an oscillatory displacement of the droplet along $\pm\hat{y}$ is observed, see Fig. 3 (Media 1).

#119442 - $15.00 USD Received 2 Nov 2009; revised 10 Dec 2009; accepted 7 Feb 2010; published 11 Mar 2010

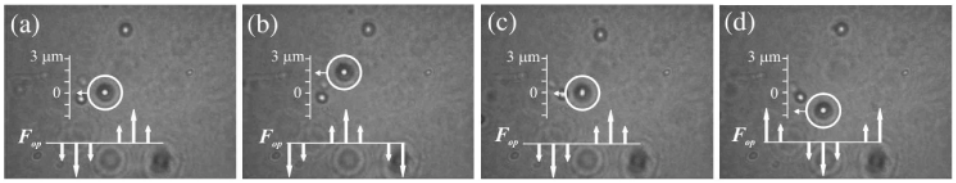

Fig. 3. Dynamics of an optically isotropic (i.e., radial) LC droplet due to the movement of the polarization pattern. For a non-rotating particle, only the optical force F_{op} occurs. The frames sequence is extracted from a movie (Media 1). Frames (a)-(d) show the droplet displacement along the y-axis induced by the spatially modulated $F_{op,y}$. Starting from a position where the $F_{op,y}$ is zero (a), the LC droplet moves up (b) and down (c)-(d) by ~2μm depending on the $F_{op,y}$ direction. The optical force field $F_{op,y}$ and the ruler are reported as guides for the eyes.

When an optically anisotropic particle, i.e. a bipolar droplet, is placed in a circular polarization fringe, due to the transfer of the angular momentum ($\vec{\tau}_{op} \neq 0$), it is set in rotation [16]. A uniform angular velocity ($\vec{\Omega}$ =const.) is reached when $\vec{\tau}_D + \vec{\tau}_{op} = \vec{0}$, where $\vec{\tau}_D = -8\pi\eta a^3 \vec{\Omega}$ is the viscous torque, a is the radius of the particle and η the fluid viscosity. The measured rotation frequency values are few Hz (2-5Hz). In this case, the translation of the polarization pattern induces an unconventional trapping of the spinning particle in the fringe, dragging it along $\pm\hat{x}$. The Fig. 4 shows the trapping of a bipolar droplet rotating clockwise in a circular polarization fringe. The shift of the polarization pattern along $-\hat{x}$ induces an equal displacement of the droplet, that preserves the clockwise rotation, see Fig. 4 (Media 2). Correspondingly, the trapping of the rotating droplet has been observed when the sample is moved with respect to the fringes, see Fig. 4 (Media 3).

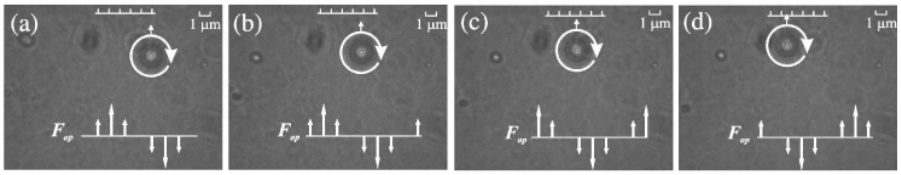

Fig. 4. Dynamics of an optically anisotropic (bipolar) LC droplet by shifting the polarization pattern. The lift force F_L traps the rotating particle in the circular polarization fringes. The frames sequence is extracted from a movie (Media 2). In the frames (a)-(d) a spinning droplet is dragged along $-\hat{x}$, due to a corresponding shift of the polarization pattern. The optical force field $F_{op,y}$ and the ruler are reported as guides for the eyes. Similar behaviour is observed when the sample is translated with respect to the polarization pattern (Media 3)

In Fig. 5, the simultaneous trapping of two particles rotating in opposite sense in two adjacent fringes is reported, see also Fig. 5 (Media 4).

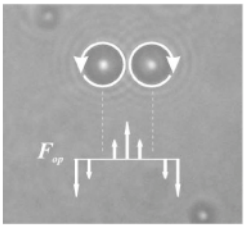

Fig. 5. Trapping of two optically anisotropic LC droplets in two adjacent fringes with opposite circular polarization. The frame is extracted from a movie (Media 4) and shows the optical trapping of two bipolar LC droplets spinning in opposite directions.

The sole optical force configuration $\vec{F}_{op}(x)$, see Eq. (7), could justify the experimental findings for the isotropic, non-rotating, LC droplets. On the other hand, the trapping of the

#119442 - $15.00 USD Received 2 Nov 2009; revised 10 Dec 2009; accepted 7 Feb 2010; published 11 Mar 2010

anisotropic particles in the circular polarization fringes, when they are set in rotation by the optical torque (8), cannot be accounted for by the mere optical force because of its null x-component. Moreover, even considering the momentum redistribution of the light after passing through the rotating birefringent droplet, the calculated optical force doesn't exhibit any x-component, which might justify the observed behaviour.

A comprehensive study of the dynamics of the LC droplets in such an optical field requires us to consider the equations of motion of spherical particles in a viscous fluid, including the hydrodynamic forces and torques. The systems typically used for optical trapping, exhibit strongly viscous behaviour governed by Stokes equations, and refer to a small Reynolds number regime [19]. Exploiting this scheme we find that besides the viscous force $\vec{F}_D = -6\pi a\eta\vec{v}$ and the optical force, a spinning particle also experiences the lift force. In the small Reynolds number regime, the lift force is $\vec{F}_L = \pi a^3 \rho\, \vec{\Omega}\times\vec{v}$ [19], where ρ is the density of the fluid. Considering typical values for the physical quantities in the $\vec{F}_L$ formula, its estimated value is two order of magnitude lower than the maximum value for $F_{op,y}$. It is only force which exhibits a x-component, and its effect is consistent with the experimental observations. In Fig. 2, together with the polarization pattern (see Fig. 2(a)), and the optical force field in the xy-plane (see Fig. 2(b)), a spherical particle rotating in clockwise sense and the corresponding streamlines of the fluid are shown (see Fig. 2(c)). Translating the polarization fringes along $\hat{x}$, the optical force along $-\hat{y}$ moves the spinning sphere in this direction. The acquired linear velocity $\vec{v}$ of the rotating particle along $-\hat{y}$ generates the lift forces on a perpendicular direction with respect to the velocity, namely $\hat{x}$, which pushes the particle towards the circular polarization fringe. This force, which originates from the different velocity of the fluid on the opposite sides of the particle (see Fig. 2(c)), known as Magnus effect [20], could represent the restoring force for the spinning particle toward the circular polarization regions. Indeed, if the polarization fringes were moved in the opposite side ($-\hat{x}$), the particle would acquire the linear velocity $\vec{v}$ along $\hat{y}$ and the lift force would occur along $-\hat{x}$. As a result of the fringes displacement, the birth of the lift force is expected, which may work as a new kind of trap for rotating particles in the polarization pattern.

4. Conclusion

Our results demonstrated that, exploiting the vectorial nature of the light, new strategies for optical trapping and manipulation can be established. Multiple and multifunctional optical traps inside an uniformly illuminated region can be created exploiting the polarization gradient. Even in the simplest geometry, i.e. interference of two orthogonally polarized beams, interesting optical manipulation features for isotropic particles emerge, as well as an unusual hydrodynamic trapping force for birefringent spinning particles. Improvements of this technique can be introduced by engineering more advanced configurations of the polarization patterns, which suggest intriguing applications in the fields of multifunctional optical manipulation, biotechnologies and optical micromachines to control motion and flows.

Acknowledgments

The authors thank V. Carbone and K. Volke-Sepulveda for discussions.

#119442 - $15.00 USD Received 2 Nov 2009; revised 10 Dec 2009; accepted 7 Feb 2010; published 11 Mar 2010